

Interaction of Bioactive Pyrazolo[4,3-*a*]acridines with Human Serum Albumin

Khosravi, Fatemeh; Pordel, Mehdi[†]; Davoodnia, Abolghasem*

Department of Chemistry, Mashhad Branch, Islamic Azad University, Mashhad, I.R. IRAN

ABSTRACT: Several heterocyclic bioactive fluorescent 3-alkyl-3H-pyrazolo[4,3-*a*]acridin-11-carbonitriles were conveniently synthesized from the reaction of 1-alkyl-1H-indazoles with different aryl acetonitrile in basic methanol solution in good yields. The interactions of 3H-pyrazolo[4,3-*a*]acridin-11-carbonitriles with Human Serum Albumin (HSA) were studied by fluorescence spectroscopy. The binding of 3-alkyl-3H-pyrazolo[4,3-*a*]acridin-11-carbonitriles quenches the HSA fluorescence, revealing a 1:1 interaction with a binding constant of about $1.28 \times 10^3 - 1.85 \times 10^3 \text{ M}^{-1}$. A decrease in fluorescence intensity at 339 nm, when excited at 295 nm, is attributed to changes in the environment of the protein fluorophores caused by the presence of the ligand. The results show that pyrazolo[4,3-*a*]acridines with R=propyl, butyl, isobutyl and R'=chlorine substituents have suitable thermodynamic and binding parameters with HSA.

KEYWORDS: 1-Alkyl-1H-indazoles; Arylacetonitriles; 3H-pyrazolo[4,3-*a*]acridin-11-carbonitriles; Human serum albumin; Interaction; Fluorescence spectroscopy.

INTRODUCTION

Human Serum Albumin (HSA) is most abundant serum protein in humans. It binds and transports a large variety of ligands including hormones, fatty acids, drugs, etc. [1–4].

HSA which is labeled with fluorescent probes is used to study of surface-induced conformational changes in protein interfaces. The binding capacity and binding sites of albumins have been characterized with many experiments. The spectral changes observed on the binding of fluorophores with proteins are important tools for the investigations of the topology of the binding sites, of the conformational changes and for the characterization of the substrate to ligand binding [5]. The determination of protein quantity in biological liquids is of great importance in biology and medicine [6] and fluorescent probes are applied for this approach [7].

Serum albumin is considered as a model for studying drug-protein interaction *in vitro*.

Recently, pyrazoles have attracted much attention because of their synthetic accessibility and their diverse chemical and biological properties are widely recognized. Some of the most important biological activities of pyrazoles are the effective antirheumatoid (SC-58635 Celecoxib), antiviral agents (Pyrazomycin), hormone oxytocin agonists (WAY VNA-932) and selective Human C1s inhibitors [8]. Additionally, the photophysical properties of pyrazoles have attracted interest in both aqueous and non-aqueous solvents as well as in various microheterogeneous media due to the possibility of Charge Transfer (CT) emission [9]. Also, as an important type of tricycle nitrogen heterocycle, acridines [10, 11]

* To whom correspondence should be addressed.

[†] E-mail: mehdipordel58@mshdiau.ac.ir

1021-9986/2017/5/85-91

8/\$/5.80

are one of the oldest classes of photoactive and bioactive compounds that are extensively used for the production of dyes and some valuable drugs. In particular, some of them are found to be efficient fluorescent chemosensors for recognition of transition metal ions such as Hg^{2+} [12] and emitters for luminescence studies [13], antibacterial [14,15], antiviral [16,17], anti prion [18], and antimalarial [19,20] agents. Some work in these areas continues, but recent research has focused mainly on their utility as anticancer [21, 22] and antitumor [23,24] drugs. This is because of the ability of the acridine chromophore to intercalate within the double-stranded DNA structure and inhibit topoisomerase enzymes.

Recently, we have synthesized some pyrazolo[4,3-*a*]acridines showed very high activity against the *Escherichia coli* HB101 (BA-7601C), *Staphylococcus aureus* (PTCC-1074), *Pseudomonas aeruginosa* (PTCC 1431), and *Bacillus subtilis* (PTCC 1365) comparable to Ampicillin and Penicillin G as reference drugs [25, 26]. Furthermore, our research on their cytotoxic action, anticancer, antitumor and antiviral activities is in progress in our laboratory. These compounds had also extremely strong fluorescence with high quantum yields [25–27]. Since detailed knowledge of the binding interaction of bioactive pyrazolo[4,3-*a*]acridines on albumin and of their relative strengths is important especially for considering such compounds as lead heterocycles for the development of novel drugs, in this paper, interactions of pyrazolo[4,3-*a*]acridine derivatives with HSA are studied by fluorescence spectroscopy. Information obtained by this work, along with the results of the biological evaluation can provide a deeper insight into the design of new 3*H*-pyrazolo[4,3-*a*]acridines with a suitable functionalization which will lead to the synthesis and the development of novel, safer and more effective drugs.

EXPERIMENTAL SECTION

Materials, methods, and instruments

Methanol, N,N-dimethylformamide (DMF), methyl iodide, ethyl bromide, *n*-propyl bromide, *n*-butyl bromide, isobutyl bromide, phenyl acetonitrile, 2-(4-chlorophenyl)acetonitrile, 2-(4-methyl phenyl)acetonitrile and 2-(4-methoxyphenyl)acetonitrile were purchased from Merck. Human serum albumin (HSA, fatty acid-free <0.05%), potassium hydroxide (KOH) and 2-(4-bromophenyl)acetonitrile were purchased from Sigma–

Aldrich. All solvents were dried according to standard procedures. Compounds **1a–e** [28] and **3a–q** [25–27] were synthesized as described in the literature.

Melting points were measured on an electrothermal type-9100 melting-point apparatus. Fluorescence measurements were performed on a Varian Cary Eclipse spectrofluorimeter. A 1.00 cm quartz cell was used for these studies. Fluorescence spectra were recorded in the range 300–550 nm, upon excitation at 295 nm for HSA. All measurements were carried out at room temperature.

General procedure for the synthesis of compounds 3a–q

1-Alkyl-5-nitro-1*H*-indazoles (**1a–e**) (10 mmol) and aryl acetonitrile **2a–e** (12 mmol) were added with stirring to a solution of KOH (13 g, 238 mmol) in methanol (50 mL). The mixture was stirred at room temperature for 24 h., The precipitate was collected by filtration after concentration at reduced pressure, washed with water, following with EtOH, and then air dried to give crude **3a–q**.

*3-Methyl-3H-pyrazolo[4,3-*a*]acridine-11-carbonitrile (3a)*
m.p.: 253–255 °C (lit.[25] m.p.: 251–253 °C).

*3-Ethyl-3H-pyrazolo[4,3-*a*]acridine-11-carbonitrile (3b)*
m.p.: 207–209 °C (lit.[25] m.p.: 209–211 °C).

*3-Propyl-3H-pyrazolo[4,3-*a*]acridine-11-carbonitrile (3c)*
m.p.: 208–210 °C (lit.[25] m.p.: 208–209 °C).

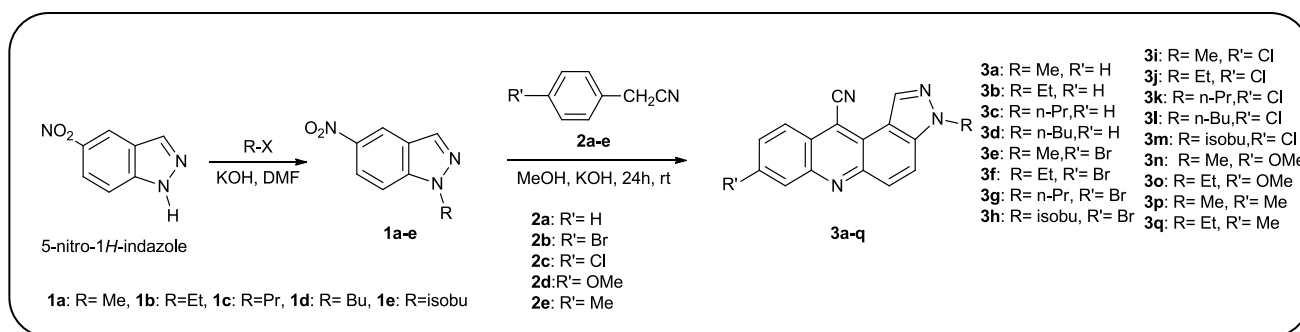
*3-Butyl-3H-pyrazolo[4,3-*a*]acridine-11-carbonitrile (3d)*
203–205 °C (lit.[25] m.p.: 200–201 °C).

*8-Bromo-3-methyl-3H-pyrazolo[4,3-*a*]acridine-11-carbonitrile (3e)*
268–270 °C (lit.[25] m.p.: 266–280 °C).

*8-Bromo-3-ethyl-3H-pyrazolo[4,3-*a*]acridine-11-carbonitrile (3f)*
231–233 °C (lit.[25] m.p.: 233–235 °C).

*8-Bromo-3-propyl-3H-pyrazolo[4,3-*a*]acridine-11-carbonitrile (3g)*
230–232 °C (lit.[25] m.p.: 228–230 °C).

*8-Bromo-3-isoButyl-3H-pyrazolo[4,3-*a*]acridine-11-carbonitrile (3h)*
190–193 °C (lit.[25] m.p.: 192–194 °C).



Scheme 1: Synthesis of compounds 3a-q.

8-Chloro-3-methyl-3H-pyrazolo[4,3-*a*]acridine-11 carbonitrile (3i).

319–321 °C (lit.[26] m.p.: 317–319 °C).

8-Chloro-3-ethyl-3H-pyrazolo[4,3-*a*]acridine-11 carbonitrile (3j)

294–296 °C (lit.[26] m.p.: 295–297 °C).

8-Chloro-3-propyl-3H-pyrazolo[4,3-*a*]acridine -11 carbonitrile (3k)

274–276 °C (lit.[26] m.p.: 273–275 °C).

3-Butyl-8-chloro-3H-pyrazolo[4,3-*a*]acridine -11- carbonitrile (3l).

263–265 °C (lit.[26] m.p.: 261–264 °C).

8-Chloro-3-isobutyl -3H- pyrazolo[4,3-*a*]acridine -11- carbonitrile (3m).

245–247 °C (lit.[26] m.p.: 245–247 °C).

8-Methoxy -3- methyl -3H- pyrazolo[4,3-*a*]acridin -11- carbonitrile (3n)

323–325 °C (lit.[27] m.p.: 325–327 °C).

3-Ethyl-8-methoxy -3H- pyrazolo[4,3-*a*]acridin -11- carbonitrile (3o)

309–311 °C (lit.[27] m.p.: 310–312 °C).

3,8-Dimethyl-3H-pyrazolo[4,3-*a*]acridin-11-carbonitrile (3p)

263–265 °C (lit.[27] m.p.: 261–264 °C).

3-Ethyl -8- methyl -3H- pyrazolo[4,3-*a*]acridin -11- carbonitrile (3q)

256–259 °C (lit.[27] m.p.: 255–256 °C).

RESULTS AND DISCUSSION

Chemistry

As depicted in Scheme 1, the synthesis of the target compounds was started with the preparation of 1-alkyl-5-nitro-1H-indazoles (**1a–e**) from 5-nitro-1H-indazole using different alkyl halides treatment in DMF and KOH according to a literature method [28]. The reaction of 1-alkyl-5-nitro-1H-indazoles with various aryl acetonitriles **2a–e** led to the formation of the 3-alkyl-3H-pyrazolo[4,3-*a*]acridine-11-carbonitriles (**3a–q**) in basic MeOH solution *via* the nucleophilic substitution of hydrogen which proceeds at room temperature with subsequent cyclization and in good yields [25–27] (Scheme 1).

Steady-state fluorescence

The interactions of bioactive 3-alkyl-3H-pyrazolo[4,3-*a*]acridine-11-carbonitriles (**3a–q**) with Human Serum Albumin (HSA) were studied by fluorescence spectroscopy. The intrinsic fluorescence of HSA with increasing concentration of **3a–q** was recorded in the range of 300–550 nm. When the concentration of HSA was fixed at 2×10^{-6} M, and the concentrations of **3a–q** were gradually increased, the fluorescence intensity of the protein band decreased. As an example, the relations of curves obtained for HSA and **3a** is presented in Fig. 1. The emission maximum shifts from 339.0 to 334.0 nm. The observations reflect that pyrazolo[4,3-*a*]acridine **3a** causes a decrease in the tryptophan fluorescence quantum yield of HSA. A blue shift in the fluorescence maximum also suggests a reduction in the polarity of the microenvironment.

To further elaborate the fluorescence quenching mechanism, the Stern-Volmer equation was used for the data analysis [29]:

$$F_0/F = 1 + K_{SV} [Q] \quad (1)$$

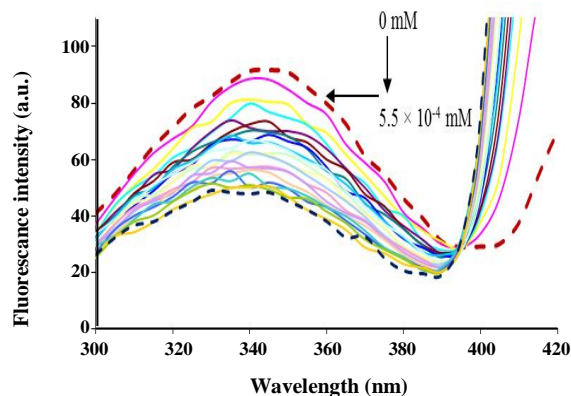


Fig. 1: Emission spectra of HSA in the presence of different concentrations of **3a**; [HSA] = 2×10^{-6} M; λ_{ex} = 295 nm; pH = 7.4.

Where F_0 and F are the steady-state fluorescence intensities in the absence and presence of quencher, respectively. K_{SV} is the Stern-Volmer quenching constant and $[Q]$ is the concentration of the quencher. The Stern-Volmer plot, showed the linear curve, upward toward y-axis at higher concentrations of **3a–q** (Fig. 2). This revealed the quenching type may be static or dynamic since the characteristic Stern-Volmer plot of combined quenching (both static and dynamic) is an upward curvature. The linear plot, however, is not adequate to describe the quenching type. Therefore, the procedure of quenching was further confirmed from the value of bimolecular quenching rate constant, k_q , which was evaluated using Eq. (2) [30]:

$$k_q = K_{SV} / \tau_0 \quad (2)$$

where τ_0 is the average lifetime of the biomolecule without quencher ($\tau_0 = 10^{-8}$ s [31]). The bimolecular quenching rate constant of **3a** was calculated to be 2.70×10^{11} L/M.s. This is largely greater than the maximum scatter collision quenching constant of the biomolecule ($K_q = 2.0 \times 10^{10}$ L/M.s) [32]. The high affinity and specificity of this interaction suggest that the quenching was mainly arisen by the formation of a non-fluorescent complex, i.e. static quenching. Table 1 shows the thermodynamic parameters of HSA–**3a–q** systems and the correlation coefficients of the plots (R^2).

Since the fluorescence quenching was a result of a static quenching mechanism, the binding constant (K_a) and the number of binding sites (n) can be determined by the following equation [32]:

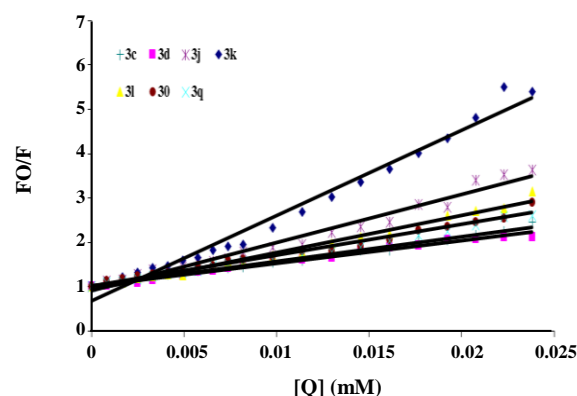


Fig. 2: Stern–Volmer plot for the binding of some pyrazolo [4,3-*a*]acridines with HSA at 25 °C.

$$\log(F_0 - F)/F = \log K_a + n \log [Q] \quad (3)$$

Where the binding constant (K_a) and the number of binding sites (n) are obtained through the ordinate and slope of the Hill curve of $\log [(F_0 - F)/F]$ versus $\log [Q]$ [33]. The binding constant (K_a) thus obtained was used to calculate the standard free energy change

$\Delta G_{\text{binding}}^0$ of the ligand binding to HSA from the relationship

$$\Delta G_{\text{binding}}^0 = -RT \ln K_a \quad (4)$$

The values of n , K_a and $\Delta G_{\text{binding}}^0$ are listed in Table 2. The values of K_a were found to be $1.28 \times 10^3 - 1.85 \times 10^3$ M⁻¹ for HSA and the values of n were noticed to be 0.84 - 1.09 at 25 °C. It was found that pyrazolo[4,3-*a*]acridines with chlorine substituent at C8-position have large K_a values. Also, the binding constant increased with increasing alkyl chain length of the alkyl substituent, resulting in the stabilization of the pyrazolo[4,3-*a*]acridines – HSA complex. All these evidence seems to indicate that pyrazolo[4,3-*a*]acridines with chlorine substituent at C8-position and propyl, butyl or isobutyl substituents at N3-position (**3k**, **3l**, **3m**) have a more stable complex with HSA than other pyrazolo[4,3-*a*]acridine derivatives.

CONCLUSIONS

In this study, the interaction of bioactive pyrazolo[4,3-*a*]acridines **3a–q** with HSA has been investigated *in vitro* under simulated physiological conditions (pH 7.4, ionic strength 10 mM) using the optical technique.

Table 1: Thermodynamic parameters of HSA–3a–q systems; R^2 represents the correlation coefficients of the plots.

Ligand	$K_{SV} \times 10^4$ (L/M)	$k_q \times 10^{12}$ (L/M s)	R^2	ΔG° (kJ/M)
3a	0.27	0.27	0.9764	-19.57
3b	0.75	0.75	0.9299	-22.11
3c	1.05	1.05	0.9404	-22.94
3d	1.02	1.02	0.9942	-22.86
3e	0.66	0.66	0.9774	-21.79
3f	0.89	0.89	0.9280	-22.53
3g	1.01	1.01	0.9899	-22.76
3h	0.95	0.95	0.9809	-22.84
3i	0.74	0.74	0.8496	-22.07
3j	1.50	1.50	0.9884	-23.82
3k	1.55	1.55	0.9853	-23.90
3l	1.40	1.40	0.9805	-23.65
3m	0.67	0.67	0.8697	-21.84
3n	0.69	0.69	0.9654	-21.90
3o	1.20	1.20	0.9824	-23.27
3p	0.51	0.51	0.9942	-21.15
3q	1.08	1.08	0.9774	-23.01

Table 2. Thermodynamic and binding parameters of HSA with 3a–q at $\lambda_{ex} = 295$ nm.

Ligand	K_a (M^{-1})	n	R^2	ΔG° (kJM^{-1})
3a	1.28×10^3	0.98	0.9722	-17.73
3b	1.31×10^3	0.94	0.9884	-17.78
3c	1.45×10^3	1.07	0.9904	-18.03
3d	1.40×10^3	1.03	0.9955	-17.94
3e	1.30×10^3	1.04	0.9673	-17.76
3f	1.37×10^3	0.89	0.9322	-17.89
3g	1.49×10^3	0.94	0.9822	-18.10
3h	1.45×10^3	0.98	0.9984	-18.03
3i	1.43×10^3	0.88	0.9612	-18.00
3j	1.41×10^3	1.01	1	-17.97
3k	1.60×10^3	0.84	1	-18.28
3l	1.80×10^3	0.86	1	-18.57
3m	1.85×10^3	0.86	0.9844	-18.64
3n	1.33×10^3	0.98	0.9898	-17.82
3o	1.38×10^3	1.07	0.9204	-17.91
3p	1.29×10^3	1.09	0.9965	-17.75
3q	1.40×10^3	1.02	0.9945	-17.94

The data of fluorescence spectroscopy indicated the changes in the microenvironment of HSA induced by the binding of **3a-q** and revealed a complex formation at 1:1 mole ratio. The results revealed that pyrazolo[4,3-a]acridines with R= propyl, butyl, isobutyl and R'=chlorine substituents have suitable thermodynamic and binding parameters with HSA.

The obtained information, along with the results of the biological evaluation can provide a deeper insight into the design of new pyrazolo[4,3-a]acridines with a suitable functionalization which will lead to the synthesis and the development of novel, safer and more effective drugs.

Received : Aug. 2, 2016 ; Accepted : Apr. 10, 2017

REFERENCES

- [1] Kratz F, Elsadek B., [Clinical Impact of Serum Proteins on Drug Delivery](#), *J. Control. Release.*, **161**:429-445 (2012).
- [2] Varshney A., Sen P., Ahmad E., Rehan M., Subbarao N., Khan R.H., [Ligand Binding Strategies of Human Serum Albumin: How Can the Cargo be Utilized?](#), *Chirality*, **22**:77-87 (2010).
- [3] Yang F., Zhang Y., Liang H., [Interactive Association of Drugs Binding to Human Serum Albumin](#), *Int. J. Mol. Sci.*, **15**:3580-3595 (2014).
- [4] Zaidi N., Ahmad E., Rehan M., Rabbani G., Ajmal M.R., Zaidi Y., Subbarao N., Khan R.H., [Biophysical Insight Into Furosemide Binding to Human Serum Albumin: A Study to Unveil its Impaired Albumin Binding in Uremia](#), *J. Phys. Chem. B.*, **117**:2595-2604 (2013).
- [5] Meireles L, Gur M, Bakan A, Bahar I., [Pre-Existing Soft Modes of Motion Uniquely Defined by Native Contact Topology Facilitate Ligand Binding to Proteins](#), *Protein Sci.*, **20**:1645-1658 (2011).
- [6] Sato T., Saito Y., Chikuma M., Saito Y., Nagai S., [Determination of Albumin in Bronchoalveolar Lavage Fluid by Flow-Injection Fluorometry Using Chromazurol S](#), *Biol. Pharm. Bull.*, **31**:336-339 (2008).
- [7] Jones L.J., Haugland R.P., Singer V.L., [Development and Characterization of the NanoOrange® Protein Quantitation Assay: A Fluorescence-Based Assay of Proteins in Solution](#). *Biotechniques*, **34**:850-861 (2003).
- [8] Meneyrol J., Follmann M., Lassalle G., Wehner V., Barre G., Rousseaux T., Altenburger J.M., Petit F., Bocskei Z., Schreuder H., Alet N., [5-Chlorothiophene-2-carboxylic Acid \[\(S\)-2-\[2-Methyl-3-\(2-oxopyrrolidin-1-yl\)benzenesulfonylamino\]-3-\(4-methylpiperazin-1-yl\)-3-oxopropyl\] Amide \(SAR107375\), a Selective and Potent Orally Active Dual Thrombin and Factor Xa Inhibitor.](#), *J. Med. Chem.*, **56**:9441-9456 (2013).
- [9] Grabowski Z.R., Rotkiewicz K., Rettig W., [Structural Changes Accompanying Intramolecular Electron Transfer: Focus on Twisted Intramolecular Charge-Transfer States and Structures.](#), *Chem. Rev.*, **103**:3899-4032 (2003).
- [10] Mohammadi Z.G., Mousavi S., Lashgari N., Badiie A., Shakiba Monireh, [Application of Sulfonic Acid Functionalized Nanoporous Silica \(sba-pr-so3h\) in the Green One-Pot Synthesis of Polyhydroacridine Libraries.](#), *Iran. J. Chem. Chem. Eng. (IJCCE)*, **32**(4): 9-16 (2013).
- [11] Marjani A.P., Khalafy J., Chitan M., Mahmoodi S., [Microwave-Assisted Synthesis of Acridine-1,8\(2h,5h\)-diones via a One-Pot, Three Component Reaction.](#), *Iran. J. Chem. Chem. Eng (IJCCE)*, **36**(2): 1-6 (2017).
- [12] Karagöz F., Güney O., Kandaz M., Bilgiçli A.T., [Acridine-Derived Receptor for Selective Mercury Binding Based on Chelation-Enhanced Fluorescence Effect.](#), *J. Lumin.*, **132**:2736-2740 (2012).
- [13] Babu V.S, Reddy H.K. [Rare Earth Nitrate Complexes with an ONO Schiff Base Ligand: Spectral, Thermal, Luminescence and Biological Studies.](#), *Iran. J. Chem. Chem. Engin. (IJCCE)*, **36**(4): 101-109 (2017).
- [14] Kaya M., Yıldırım Y., Çelik G.Y., [Synthesis, Characterization, and In Vitro Antimicrobial and Antifungal Activity of Novel Acridines](#), *Pharm. Chem. J.*, **48**:722-726 (2015).
- [15] Denny W.A., [Acridine Derivatives as Chemotherapeutic Agents](#), *Curr. Med. Chem.*, **9**:1655-1665 (2002).
- [16] Goodell J.R., Madhok A.A., Hiasa H., Ferguson D.M., [Synthesis and Evaluation of Acridine-and Acridone-Based Anti-Herpes Agents with Topoisomerase Activity](#), *Bioorg. Med. Chem.*, **14**:5467-5480 (2006).

- [17] Tabarrini O., Manfroni G., Fravolini A., Cecchetti V., Sabatini S., De Clercq E., Rozenski J., Canard B., Dutartre H., Paeshuysse J., Neyts J., [Synthesis and Anti-BVDV Activity of Acridones As New Potential Antiviral Agents 1](#), *J. Med. Chem.*, **49**:2621-2627 (2006).
- [18] Kukowska-Kaszuba M., Dzierzbicka K., [Synthesis and Structure-Activity Studies of Peptide-Acridine/Acridone Conjugates](#), *Curr. Med. Chem.*, **14**: 3079-3104 (2007).
- [19] Winter R.W., Kelly J.X., Smilkstein M.J., Dodean R., Hinrichs D., Riscoe M.K., [Antimalarial Quinolones: Synthesis, Potency, and Mechanistic Studies](#), *Exp. Parasitol.*, **118**:487-497 (2008).
- [20] Joshi A.A., Viswanathan C.L., [Recent Developments in Antimalarial Drug Discovery](#), *Antiinfect. Agents Med. Chem.*, **5**:105-122 (2006).
- [21] Belmont P., Bosson J., Godet T., Tiano M., [Acridine and Acridone Derivatives, Anticancer Properties and Synthetic Methods: Where are We Now?](#), *Anticancer Agents Med. Chem.*, **7**: 139-169 (2007).
- [22] Kamal A., Srinivas O., Ramulu P., Ramesh G., Kumar P.P., [Synthesis of C8-Linked Pyrrolo \[2, 1-c\] \[1, 4\] Benzodiazepine-Acridone/Acridine Hybrids as Potential DNA-Binding Agents](#), *Bioorg. Med. Chem. Lett.*, **14**:4107-4111 (2004).
- [23] Demeunynck M., [Antitumour Acridines](#), *Expert Opin. Ther. Pat.*, **14**:55-70 (2004).
- [24] Niemira M, Dasty J, Mazerska Z., [Pregnane X Receptor Dependent up-Regulation of CYP2C9 and CYP3A4 in Tumor Cells by Antitumor Acridine Agents, C-1748 and C-1305, Selectively Diminished under Hypoxia](#), *Biochem. Pharmacol.*, **86**: 231-241 (2013).
- [25] Daghigh L.R, Pordel M., Davoodnia A., [Synthesis of New Fluorescent Pyrazolo \[4, 3-a\] Acridine Derivatives Having Strong Antibacterial Activities](#), *J. Chem. Res.*, **38**: 202-207 (2014).
- [26] Rahmani Z., Pordel M., Davoodnia A., [Design, Synthesis, Fluorescence Properties and Antibacterial Activities of New 8-Chloro-3-Alkyl-3H-Pyrazolo\[4,3-a\]acridine-11-Carbonitriles](#), *Bull. Korean Chem.*, **35**: 551-556 (2014).
- [27] Pakjoo V., Roshani M., Pordel M., Hoseini T., [Synthesis of New Fluorescent Compounds from 5-Nitro-1H-Indazole](#), *Arkivoc.* **9**: 195-203 (2012).
- [28] Bouissane L., El Kazzouli S., Léger J.M., Jarry C., Rakib E.M., Khouili M., Guillaumet G., [New and Efficient Synthesis of bi-and Trisubstituted Indazoles](#), *Tetrahedron*, **61**: 8218-8225 (2005).
- [29] Nitzan A., Jortner J., Kommandeur J., Drent E., [A Quantum Mechanical Analogue of the Stern-Volmer Equation](#), *Chem. Phys. Lett.*, **9**: 273-278 (1971).
- [30] Boaz H., Rollefson, G.K., [The Quenching of Fluorescence. Deviations from the Stern-Volmer Law](#), *J. Am. Chem. Soc.*, **72**: 3435-3443 (1950).
- [31] Lakowicz J.R., Weber G., [Quenching of Protein Fluorescence by Oxygen. Detection of Structural Fluctuations in Proteins on the Nanosecond Time Scale](#), *Biochemistry*, **12**: 4171-4170 (1973).
- [32] Gao H., Lei L., Liu J., Kong Q., Chen X, Hu Z., [The Study on the Interaction between Human Serum Albumin and a New reagent with Antitumour Activity by Spectrophotometric Methods](#), *J. Photochem. Photobiol. A: Chem.*, **167**: 213-221 (2004).
- [33] Lakowicz J.R., "Principles of Fluorescence Spectroscopy", 2nd ed Kluwer Academic/Plenum Publishers New York NY USA, (1999).